# Complete Double Epoxidation of Divinylbenzene Using Mn(porphyrin)-Based Porous Organic Polymers

Kainan Zhang, Omar K. Farha,* Joseph T. Hupp,* and SonBinh T. Nguyen*

Department of Chemistry and International Institute for Nanotechnology, Northwestern University, 2145 Sheridan Road, Evanston, Illinois 60208-3113, United States

Ⓢ *Supporting Information*

ABSTRACT: A series of porphyrin-based porous organic polymers (PPOPs) were synthesized in excellent yields via the Yamamoto−Ullmann couplings of tetrabromo spirobifluorene with several brominated porphyrin monomers. After isolation and demetalation, the metal-free PPOP can be postsynthetically metalated to form a Mn[III]−PPOP that is catalytically active toward the selective double-epoxidation of divinylbenzene to divinylbenzene dioxide.
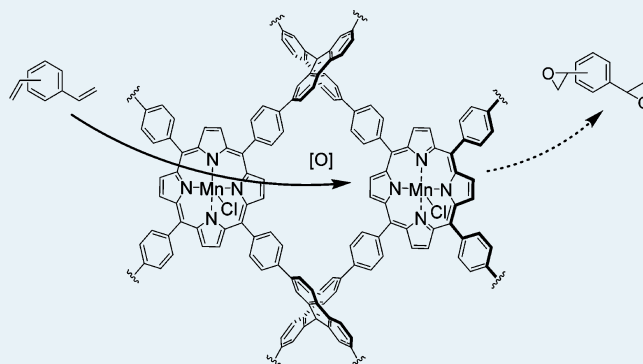
KEYWORDS: *Mn(porphyrin), porous organic polymer, epoxidation, divinylbenzene, divinylbenzene dioxide*

The synthesis of multiepoxides from available multiolefin precursors is a key process in the preparation of epoxy resins, a class of technologically important materials with excellent mechanical and electrical insulating properties as well as good resistances to chemicals and temperature.[1] Among the multiepoxides that are currently in use, divinylbenzene dioxide (DVBDO) is an important popular and high-tech component in epoxy thermoset formulations for use as coatings, structural components, and modeling composites.[2] Yet to date, there are only a handful of catalytic processes reported for the preparation of DVBDO,[3−5] often with low conversion and broad product mixtures.[2,4−6] Thus, a catalyst that can epoxidize divinylbenzene (DVB) to DVBDO with good conversion and selectivity is highly desirable. Herein, we report a porous organic polymer (POP) catalyst that can successfully accomplish this goal through a microporous environment with multiple catalyst entities that can encapsulate DVB and oxidize both of its olefin groups.

Although metalloporphyrins have been intensively studied as epoxidation catalysts, given their high activities and close biological relevance to natural enzymes,[7−13] their utilities in homogeneous epoxidation have been rather limited because of several deactivation pathways, such as dimerization[13] and self-oxidation.[14] To achieve more stabilized and active catalytic systems, metalloporphyrins have been anchored to solid supports[15] as well as integrated into porous materials, such as metal organic frameworks[16−20] and porous organic polymers (POPs).[21−31] In particular, the integration of metalloporphyrins into porous frameworks has been found to lead to unexpected benefits, such as shape and size selectivity[26,32] and increases in reaction rate as a result of preconcentration effects.[29] It is this latter effect that prompted us to examine the double epoxidation of DVB inside a microporous metalloporphyrin-based POP. We hypothesize that a preconcentration of DVB inside the pores of an appropriately designed metalloporphyrin-based POP would lead to its complete double epoxidation because of the ability of adjacent catalyst moieties to interact with both vinyl functionalities. As shown below, this is, indeed, the case: excellent catalytic reactivity and high selectivity can be achieved for the double epoxidation of DVB to DVBDO using a microporous POP derived from spirobifluorene and porphyrin-based building blocks.

Although metalloporphyrins have previously been incorporated into POPs[22,31] and used for sulfide oxidation, alkene expoxidation,[31] and hydrogen peroxide decomposition,[33] these early materials have relatively moderate surface areas, which limit the range of substrates and oxidants that can be used. To overcome these limitations, we selected the spirobifluorene monomer **A** as the structure-directing comonomer in our synthesis of porphyrin-based POPs (PPOPs) using Yamamoto−Ullmann couplings,[34−38] given its tendency to afford POP materials with excellent thermostability, high microporosity, and moderate mesoporosity (based on the pore size distribution data, there are micropores at about 7 and 12 Å and a broad hump in the mesoporous region ranging from 20 to 40 Å).[34−37] For the porphyrin components, we examined both the dibromide derivatives **1** and the tetrabromide
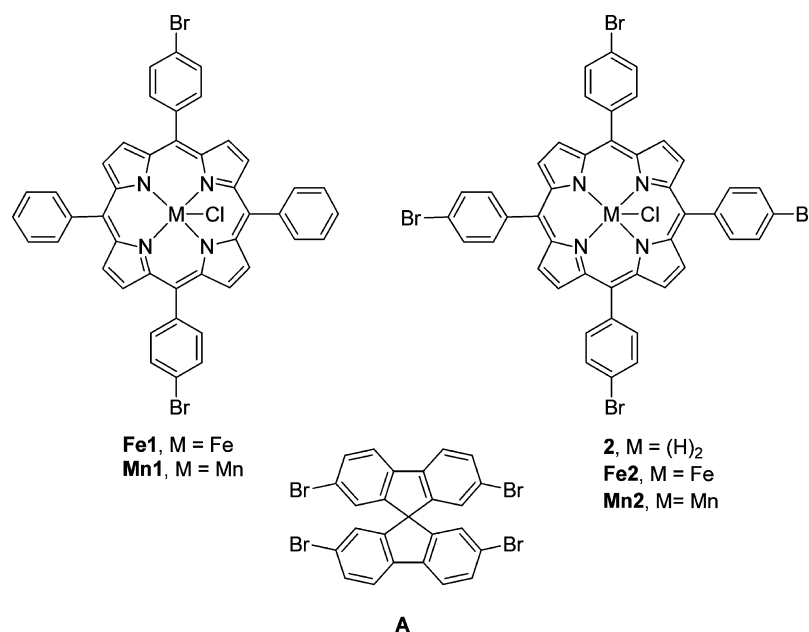
Figure 1. Monomers for Yamamoto−Ullmann coupling.

derivatives **2** (Figure 1). Curiously, although the couplings between **A** and either the free-base porphyrins (**1** and **2**) or the Fe(porphyrin) monomers (**Fe1** and **Fe2**) under various stoichiometric ratios proceed in good yields (see Supporting Information (SI)), the analogous couplings with the Mn-(porphyrin) monomers failed. Presumably, the Ni(COD)$_2$ reagent may have been oxidized by the Mn^{III} center, leading to deactivation.

As is common in Yamamoto−Ullmann couplings, a strong acidic workup is required to remove all the Ni side products. Upon this acidic workup, the Fe-containing PPOPs A_n**Fe1** and A_n**Fe2** (subscript $n = 1$−3, indicating the relative stoichiometry of **A** vs those for **Fe1** and **Fe2**), readily demetallate to form partially metalated or fully demetalated PPOPs (Scheme 1, Table 1). Complete demetalation can be achieved by a second acid treatment at 85 °C, giving rise to the corresponding free-base PPOPs $^{fb}A_n$**Fe1** and $^{fb}A_n$**Fe2**. In general, increasing the ratio of spirobifluorene **A** to the porphyrin monomers led to increases in the specific surface areas (ssa's) (Table 1, cf. entries 1−3 and entries 4−6) of the resulting free-base PPOPs. Presumably, this can be attributed to a higher degree of cross-linking possible in **A**-rich formulations.

Interestingly, A_2**2**, the PPOP derived from the free-base porphyrin monomer **2** still retains a significant amount of Ni after workup (see Table S1, entry 6 in the SI), presumably as a result of in situ metalation by the NiBr$_2$ side products. Nevertheless, most of the Ni contaminants can be removed upon a second, more rigorous acid treatment at higher temperatures (85 °C and 10 h) yielding a free-base PPOP ($^{fb}A_2$**2**) with BET surface area (Table 1, entry 7) and total pore volume that are almost twice those of $^{fb}A_2$**Fe2**, the demetalated free-base PPOP derived from A_2**Fe2**, which has the same spirobifluorene/porphyrin stoichiometry (Table 1, cf. entries 5 and 7). As expected for a material with aromatic C−C connections, PPOP $^{fb}A_2$**2** is highly stable: it retains a high surface area (1540 m^2/g) after being exposed to either concentrated hydrochloric acid or 4 M aqueous sodium hydroxide (see Figure S56 in the SI).

Metalation of both $^{fb}A_2$**2** and $^{fb}A_2$**Fe2** with MnCl$_2$·4H$_2$O$^{39-45}$ was carried out under previously established conditions^{31} (Scheme 1). Interestingly, $^{fb}A_2$**Fe2** can be metalated near quantitatively, but $^{fb}A_2$**2** is metalated only to about 67%. Treating this metalated material with additional MnCl$_2$·4H$_2$O under the same conditions does not lead to any further increase in metal loadings. Consistent with this observation, the diffuse-reflectance UV−vis spectrum of the **Mn-$^{fb}A_2$2** material (Figure S61 in the SI) also shows residual bands due to nonmetalated materials.

Metalation only moderately decreases the surface areas for **Mn-$^{fb}A_2$2** and **Mn-$^{fb}A_2$Fe2** from the parent free-base PPOP (Figure 2; Table 1, cf. entries 3 vs 8 and 7 vs 9, respectively). Notably, **Mn-$^{fb}A_2$2** retained most of the mesoporosity of the parent PPOP (Figure 3), which would be beneficial in applications such as catalysis in which mass-transport limitation can be quite important. However, the pore size distribution data for **Mn-$^{fb}A_2$Fe2** shows almost complete reduction of mesoporosity (Figure 3), a fact that is supported by a reduction of the hysteresis in the N$_2$ isotherms (Figure 2). Nevertheless, the dominant remaining micropore (∼11 Å) for this material is still large enough for DVB (∼7 Å) and DVBDO (∼9 Å) to access.

Mn-$^{fb}A_2$2 was then evaluated as a catalyst for the epoxidation reaction of styrene and DVB in the presence of 2-(tert-butylsulfonyl)iodosylbenzene (**5**) oxidant (Scheme 2).^{31,46,47} As shown in Figure 4, the epoxidation of styrene affords a good yield (80%) of styrene oxide with no significant mass loss (see Figure S63 in the SI for the NMR spectra of the reaction mixture). This is in stark contrast to the homogeneous (TPP)MnCl analogue (TTP = meso-tetraphenylporphyrinato dianion), which affords a lower yield of styrene oxide in addition to the overoxidized product benzaldehyde and the isomerization product phenyl acetylaldehyde. This homogeneous catalyst also decomposed much more easily, as shown by the change in the conversion profile after ∼15 h (Figure 4).

Consistent with the aforementioned promising styrene oxidation results, both **Mn-$^{fb}A_2$2** and **Mn-$^{fb}A_2$Fe2** show comparable good yields and selectivities toward the complete

Scheme 1. A Schematic Illustration of PPOP Synthesis and Subsequent Demtallation and Metallation
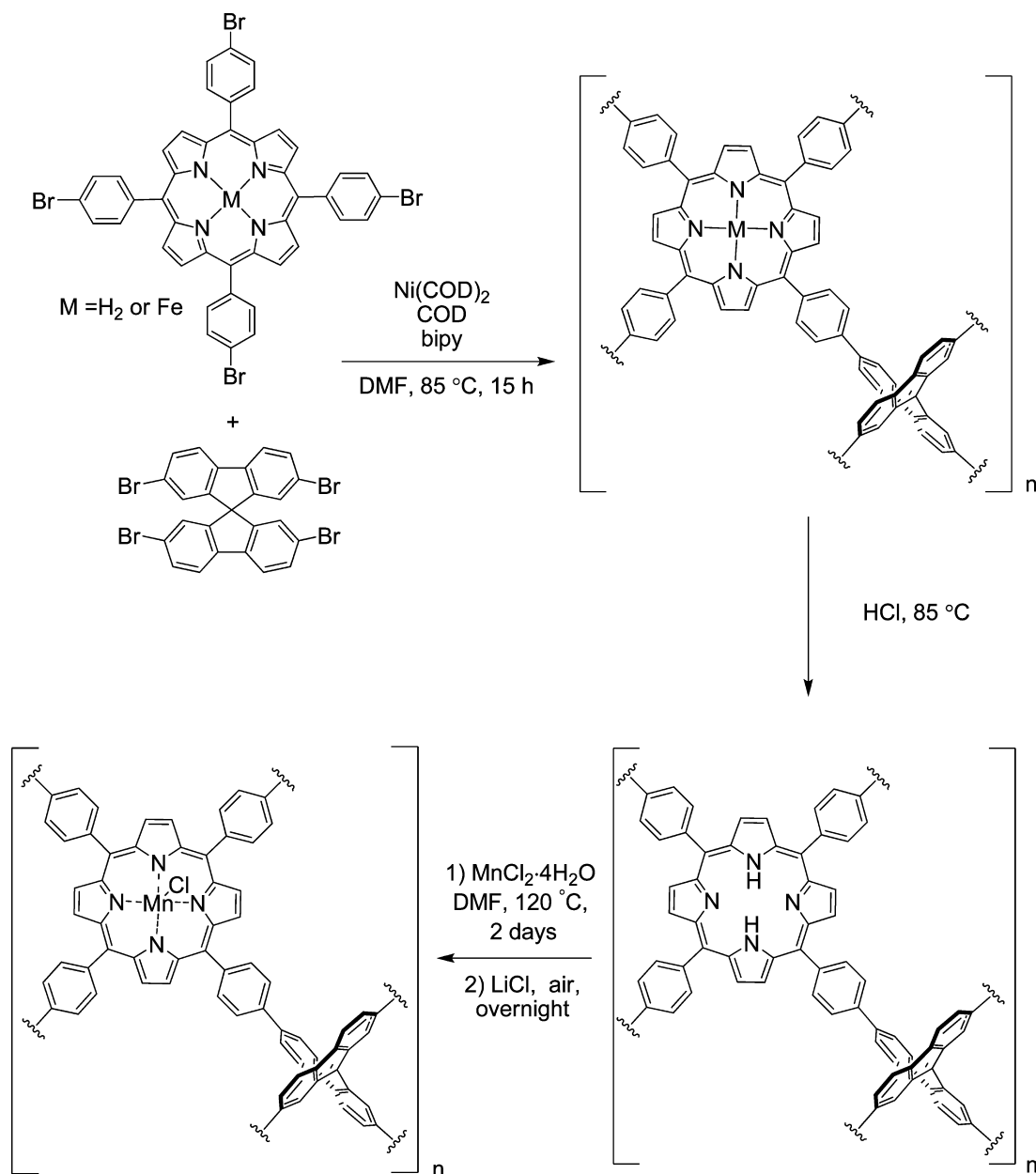

Table 1. Characterization Data for Free-Base PPOPs and Mn-PPOPs

entries	PPOPs	surface area (m²/g)	total pore volume (cm³/g)	metal loading (wt %)
1	^{fb}AFe1	760	0.35	<0.1
2	^{fb}A₂Fe1	690	0.26	0.16
3	^{fb}A₃Fe1	1130	0.46	0.14
4	^{fb}AFe2	620	0.23	0.37
5	^{fb}A₂Fe2	1120	0.57	<0.1[a]
6	^{fb}A₃Fe2	1390	0.64	<0.1
7	^{fb}A₂2	1880	0.94	0.35[b]
8	Mn-^{fb}A₂Fe2	850	0.36	4.0
9	Mn-^{fb}A₂2	1600	0.79	2.7

[a]As synthesized without further demetalation. [b]Ni content.

expoxidation of DVB to DVBDO, with >50% yield based on DVB (Scheme 3; Figure 5 and Figure S74 in the SI). Only a

trace (10 mol %) of the incomplete oxidation product divinylbenzene monoxide (DVBMO) was found, and no epoxide ring-opening product was observed (Figure 5). A moderate amount (∼24 mol %) of overoxidation product (benzylaldehyde derivative) exists at the end of the reaction, which may arise from the oxidative cleavage of the phenyl-acetylaldehyde derivative (Scheme 4).[48−50]

The advantages of the PPOP environment for DVB double epoxidation clearly stand out over its homogeneous analog (TPP)MnCl. Under the same reaction conditions (see the SI for reaction details), the homogeneous catalyst afforded a much poorer substrate conversion (Figure 6), with ∼30% of the alkene left in the reaction mixture after 30 h. In addition, GC/MS analysis shows that the major product is the partially epoxidized product DVBMO (DVBDO/DVBMO = 2:3). We attribute the higher selectivity for DVBDO in reactions catalyzed by **Mn-^{fb}A₂2** to the high concentrations of catalyst inside its pore: after DVB entered the pore of a PPOP particle
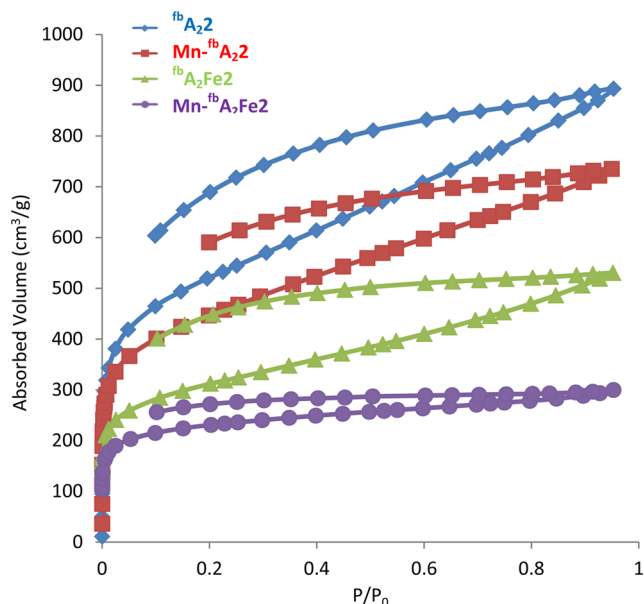
Figure 2. Stacked N_2 isotherm data for $^{fb}A_2 2$ (blue), Mn-$^{fb}A_2 2$ (red), $^{fb}A_2 Fe2$ (green), and Mn-$^{fb}A_2 Fe2$ (purple).
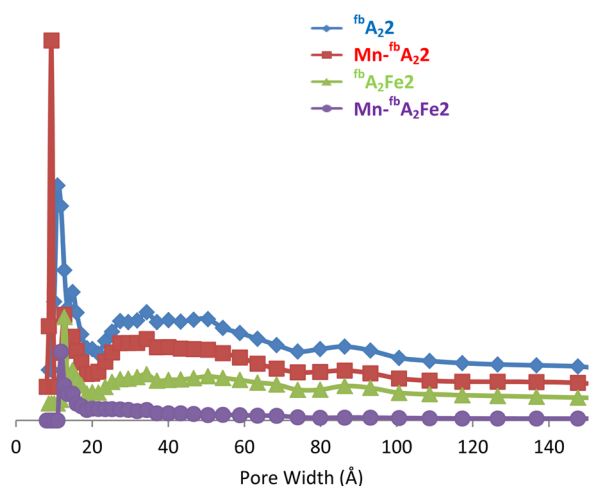

Figure 3. Stacked NLDFT (nonlocal density functional theory) pore size distribtions for $^{fb}A_2 2$ (blue), Mn-$^{fb}A_2 2$ (red), $^{fb}A_2 Fe2$ (green), and Mn-$^{fb}A_2 Fe2$ (purple). These pore size distributions are stacked by moving ~0.005 cm³ up and down for clarity. These single data can be seen in the SI with the unit on the *y* axis as incremental pore volume.

and became oxidized, the DVBMO product was still encapsulated inside the particle and had a good chance to encounter a second metal oxo moiety prior to exiting the POP particle. Such a multicatalyst environment obviously does not exist in a reaction catalyzed by the homogeneous (TPP)MnCl catalyst where DVBMO is the major product.

When DVBMO is used as the substrate (Scheme 5), its epoxidation by Mn-$^{fb}A_2 2$ proceeds at a rate and conversion similar to that of the styrene epoxidation, indicating that the presence of the *para*-epoxy functional group does not significantly affect the epoxidation of the remaining styrenic C=C bond. However, there were almost no unidentified products: DVBDO was formed in 76% yield, benzaldehyde derivatives were formed in 18% yield, and the phenyl-acetaldehyde products constituted the remainder of the mass balance (Figure 7). As in the case for DVB oxidation, the

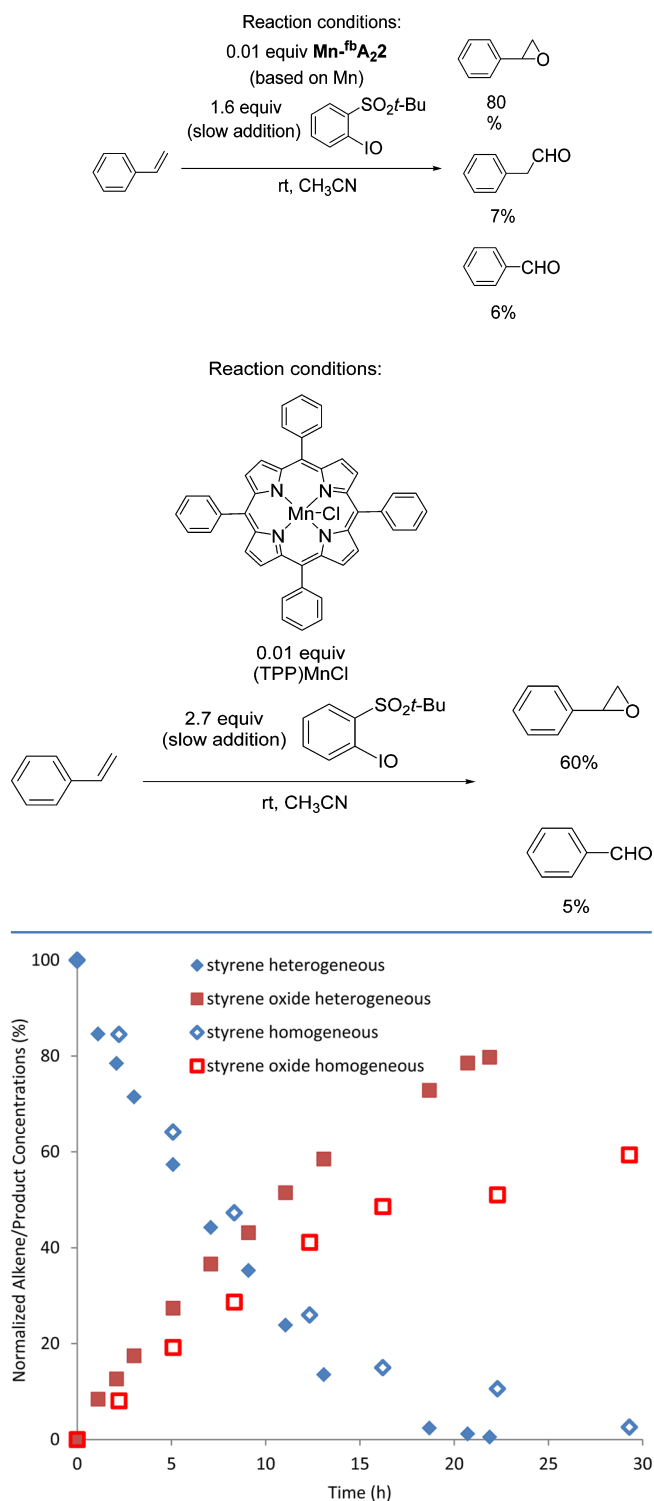**Scheme 2. Epoxidation of Styrene by Mn-$^{fb}A_2 2$ (top) and (TPP)MnCl (bottom)**

Figure 4. Comparison of styrene epoxidation using Mn-$^{fb}A_2 2$, and (TPP)MnCl.

isomerized phenylacetaldehyde products formed rather quickly, maximized at ~8 h, and then decreased. The benzaldehyde product does not form until after phenylacetaldehyde has built up, suggesting that most of the overoxidation comes from isomerization. Together with the data shown in Figure 5, these results indicate that the 20% of unidentified mass in the
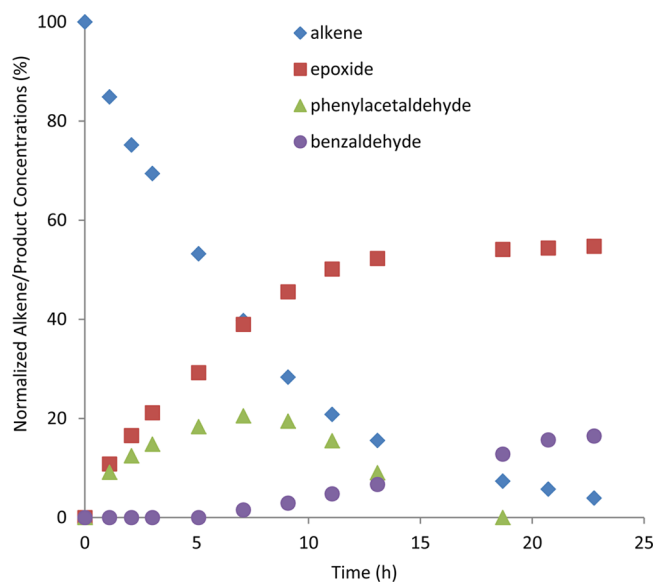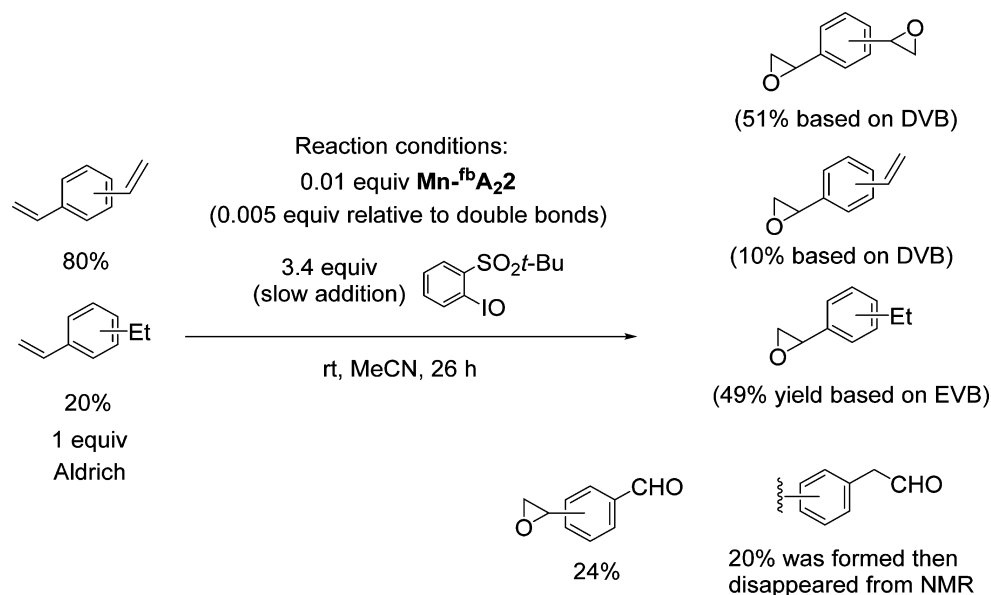
Scheme 3. Epoxidation of DVB by Mn-^{fb}A$_2$2

(51% based on DVB)

(10% based on DVB)

(49% yield based on EVB)

24%

20% was formed then disappeared from NMR

Reaction conditions:
0.01 equiv **Mn-^{fb}A$_2$2**
(0.005 equiv relative to double bonds)

3.4 equiv (slow addition)

rt, MeCN, 26 h

80%

20%
1 equiv
Aldrich

Figure 5. Plots of normalized concentrations of alkene, epoxide, phenyl acetaldehydes, and benzaldehydes as functions of time in the epoxidation DVB by **Mn-^{fb}A$_2$2**. At the end of the reaction, ∼20% of the reaction mass was compounds that could not be identified and thus was not accounted for in these plots. These compounds are attributed to potential side reactions of DVB (see further discussion below). The corresponding plots for **Mn-^{fb}A$_2$Fe2** can be found in Figure S74 in the SI.

Scheme 4. Proposed Overoxidation Pathway

oxidative cleavege
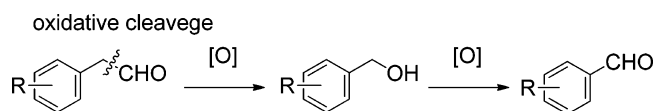
epoxidation of DVB can be attributed to its higher susceptibility to other side reactions such as alkene polymerization in the presence of Mn centers with unpaired electrons.[51−54]

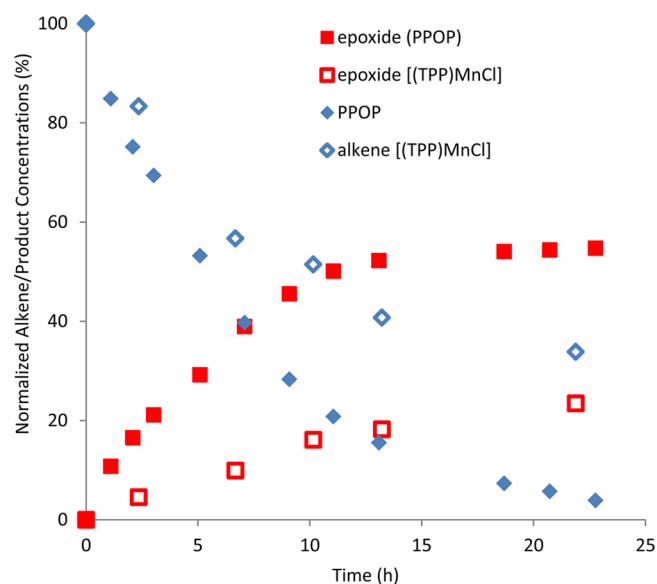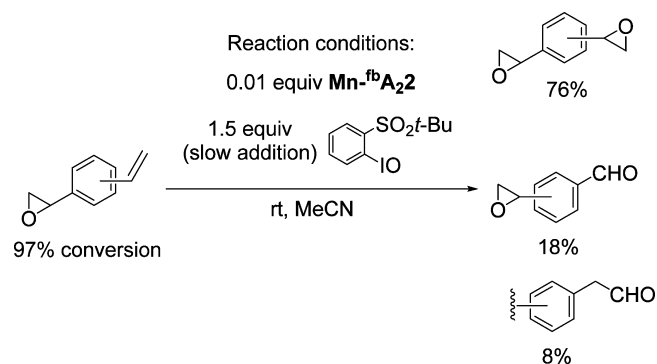The conversion and selectivity of metalloporphyrin-catalyzed epoxidation reaction can be enhanced by the addition of

Figure 6. Plots of normalized concentrations of alkene and epoxide in the epoxidation of DVB by **Mn-^{fb}A$_2$2** and (TPP)MnCl.

Scheme 5. Epoxidation of DVBMO by Mn-^{fb}A$_2$2

Reaction conditions:
0.01 equiv **Mn-^{fb}A$_2$2**

1.5 equiv (slow addition)

rt, MeCN

97% conversion

76%

18%

8%

additives such as imidazole or pyridine that can coordinate to the Mn center.[41,42,54,55] This is also the case for **Mn-^{fb}A$_2$2**: in
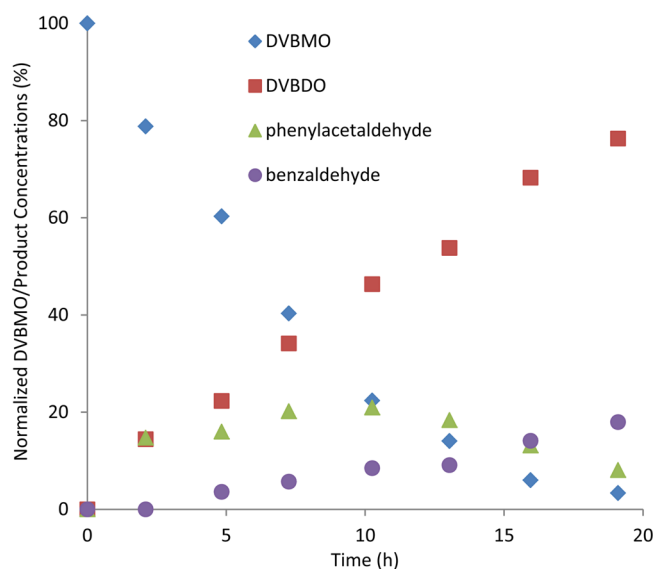
Figure 7. Plots of normalized concentrations of alkene, epoxide, phenylacetaldehyde, and benzaldehyde derivatives as functions of time in the epoxidation of DVBMO by **Mn-^{fb}A$_2$2**.

Figure 8. Normalized alkene concentration and epoxide yield for comparison of DVB epoxidation with and without imidazole.

the presence of imidazole, the overall epoxide yield is increased by an additional 19% (20% increase for overall DVBDO yield; see Scheme 6). This increase in yield can be attributed to the ability of imidazole to significantly inhibit the formation of isomerized and overoxidized byproducts (from 24% to 15% for benzaldehyde) (see Figure S69 in the SI); the maximum phenylacetaldehyde yield during the reaction is down from 20% to 6% at around 7 h (see Figure S69 in the SI). Presumably, the coordination of imidazole to the Mn(porphyrin) significantly reduces its Lewis acidity and, thus, isomerization and overoxidation (Figure 8).[56,57]

The time-dependent selectivity profile for the epoxidation of DVB catalyzed by [**Mn-^{fb}A$_2$2** + imidazole] (Figure 9) shows an early formation of DVBMO that begins to decrease after ~9 h as DVBDO becomes dominant; however, the combined amounts of DVBMO and DVDBO up to this point are much
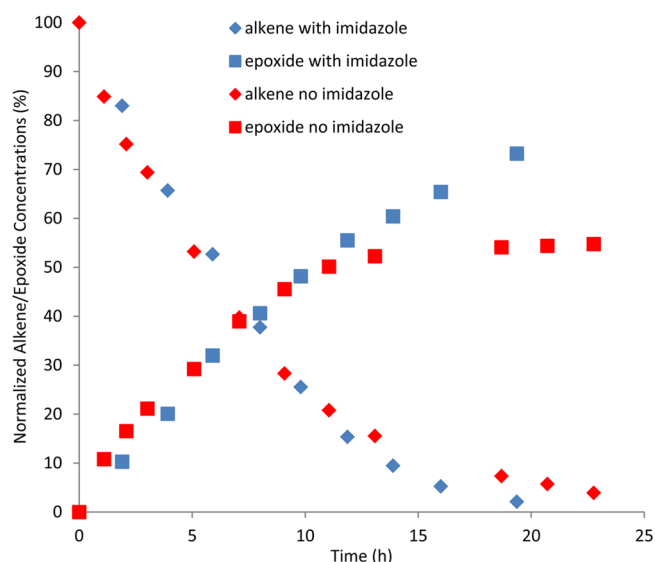
less than the amount of converted DVB, suggesting that both DVB and the initially epoxidized DVBMO are preferentially trapped inside the pores. In this manner, there is a good chance for DVB to encounter more than one catalytic site before being released into the solution and being detected as either DVBMO or DVBDO. Indeed, DVBDO was not observed until 4 h into the reaction. Together, these data further support our aforementioned hypothesis that the multicatalyst porous environment is quite crucial for the selective double epoxidation of DVB. Interestingly, the effect of imidazole in the presence of **Mn-^{fb}A$_2$Fe2** is much less than that for **Mn-^{fb}A$_2$2** (see Figure S75 in the SI). We attributed this to the lesser likelihood of the smaller pores in the latter materials to accommodate the additional imidazole ligands; that is, the smaller pores may destabilize the imidazole complex more.

It is important to note that recycling catalytic experiments are informative; however, we were unable to recycle this

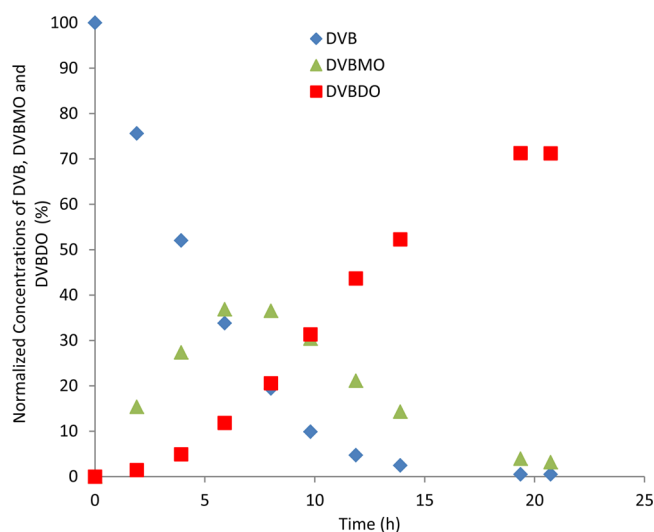**Scheme 6. Epoxidation of DVB by Mn-^{fb}A$_2$2 with Imidazole**
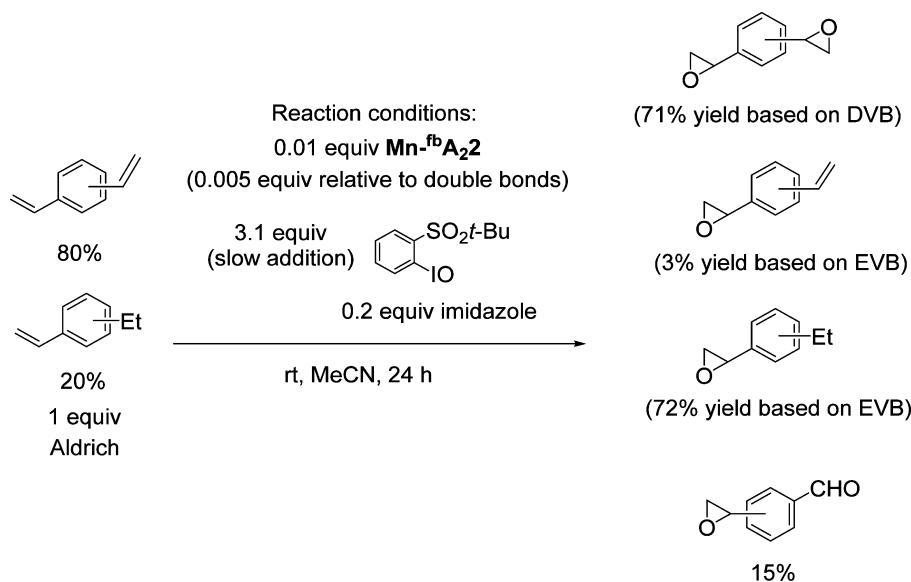
Figure 9. Plots of normalized DVB concentration, DVBDO yield (based on DVB), and DVBMO yield (based on DVB) as a function of time for the reaction in Scheme 6.

catalyst because the oxidant byproduct *tert*-butylsulfonyliodobenzene in the reaction was well mixed with the catalyst; the latter is actually the major part. Even after washing, we could not get clean catalysts, and we lost most of it during the washing process due to its fine powder form.

In summary, we have demonstrated the synthesis of a highly robust porphyrin-based POP material with good surface areas that can be readily metalated with Mn^{III} and then used for the selective double epoxidation of DVB to DVBDO in the presence of 2-(*tert*-butylsulfonyl)iodosylbenzene. Together with reaction profiling, comparative studies against the analogous homogeneous catalyst (TPP)MnCl suggest that the multicatalyst porous nature of the **Mn-^{fb}A$_2$2** material is the primary factor responsible for this successful double epoxidation. Such observations clearly set porous catalyst materials apart from other catalysts in which the high concentration of catalyst inside the pore plays a significant role in reaction outcome and selectivity.

■ ASSOCIATED CONTENT

ⓈSupporting Information

The Supporting Information is available free of charge on the ACS Publications website at DOI: 10.1021/acscatal.5b01388.

> Procedure for synthesis of PPOPs, the material characterizations, and procedures for conducting catalytic experiments (PDF)

■ AUTHOR INFORMATION

Corresponding Authors
*E-mail: o-farha@northwestern.edu.
*E-mail: j-hupp@northwestern.edu.
*E-mail: stn@northwestern.edu.

Notes
The authors declare no competing financial interest.

■ ACKNOWLEDGMENTS

■ REFERENCES

(1) Clayton, A. M. *Epoxy Resins: Chemistry and Technology*, 2nd ed.; CRC Press: New York, 1988.

(2) Gulyas, G.; Bharadwaj, A. R.; Wright, R. J.; Null, M. J.; Ripplinger, E. B. Patent WO 2011056381, May 12, 2012.

(3) Inoue, M.; Nakayama, E.; Nakamura, Y.; Rengakuji, S.; Nishibe, K. *Bull. Chem. Soc. Jpn.* **1991**, *64*, 3442−3444.

(4) Worzakowska, M. *J. Appl. Polym. Sci.* **2007**, *103*, 462−469.

(5) Marks, M. J.; Gulyas, G.; Frazier, K. A. Patent WO 2010077483, July 8, 2010.

(6) Liao, Z. K.; Boriack, C. J. U.S. Patent US6087513, July 11, 2000.

(7) Che, C. M.; Huang, J. S. *Chem. Commun.* **2009**, 3996−4015.

(8) Dolphin, D.; Traylor, T. G.; Xie, L. Y. *Acc. Chem. Res.* **1997**, *30*, 251−259.

(9) Groves, J. T.; Haushalter, R. C.; Nakamura, M.; Nemo, T. E.; Evans, B. J. *J. Am. Chem. Soc.* **1981**, *103*, 2884−2886.

(10) Groves, J. T.; Nemo, T. E.; Myers, R. S. *J. Am. Chem. Soc.* **1979**, *101*, 1032−1033.

(11) Gunter, M. J.; Turner, P. *Coord. Chem. Rev.* **1991**, *108*, 115−161.

(12) Katsuki, T. *Coord. Chem. Rev.* **1995**, *140*, 189−214.

(13) Meunier, B. *Chem. Rev.* **1992**, *92*, 1411−1456.

(14) Chang, C. K.; Kuo, M. S. *J. Am. Chem. Soc.* **1979**, *101*, 3413−3415.

(15) Bedioui, F. *Coord. Chem. Rev.* **1995**, *144*, 39−68.

(16) Zou, C.; Zhang, T. F.; Xie, M. H.; Yan, L. J.; Kong, G. Q.; Yang, X. L.; Ma, A.; Wu, C. *Inorg. Chem.* **2013**, *52*, 3620−3626.

(17) Feng, D. W.; Gu, Z. Y.; Li, J. R.; Jiang, H. L.; Wei, Z. W.; Zhou, H. C. *Angew. Chem., Int. Ed.* **2012**, *51*, 10307−10310.

(18) Corma, A.; Garcia, H.; Llabrés i Xamena, F. X. *Chem. Rev.* **2010**, *110*, 4606−4655.

(19) Lee, J.; Farha, O. K.; Roberts, J.; Scheidt, K. A.; Nguyen, S. T.; Hupp, J. T. *Chem. Soc. Rev.* **2009**, *38*, 1450−1459.

(20) Yoon, M.; Srirambalaji, R.; Kim, K. *Chem. Rev.* **2012**, *112*, 1196−1231.

(21) Zhang, Y.; Ying, J. *ACS Catal.* **2015**, *5*, 2681−2691.

(22) Kaur, P.; Hupp, J. T.; Nguyen, S. T. *ACS Catal.* **2011**, *1*, 819−835.

(23) Costa, A. A.; Ghesti, G. F.; de Macedo, J. L.; Braga, V. S.; Santos, M. M.; Dias, J. A.; Dias, S. C. L. *J. Mol. Catal. A: Chem.* **2008**, *282*, 149−157.

(24) Poltowicz, J.; Haber, J. *J. Mol. Catal. A: Chem.* **2004**, *220*, 43−51.

(25) Chen, L.; Yang, Y.; Jiang, D. L. *J. Am. Chem. Soc.* **2010**, *132*, 9138−9143.

(26) Farha, O. K.; Shultz, A. M.; Sarjeant, A. A.; Nguyen, S. T.; Hupp, J. T. *J. Am. Chem. Soc.* **2011**, *133*, 5652−5655.

(27) Hitomi, Y.; Mukai, H.; Ohyama, J.; Shinagawa, M.; Shishido, T.; Tanaka, T. *Chem. Lett.* **2007**, *36*, 660−661.

(28) Jeong, E. Y.; Ansari, M. B.; Park, S. E. *ACS Catal.* **2011**, *1*, 855−863.

(29) Shultz, A. M.; Farha, O. K.; Hupp, J. T.; Nguyen, S. T. *J. Am. Chem. Soc.* **2009**, *131*, 4204−4205.

(30) Zhang, Z. J.; Zhang, L. P.; Wojtas, L.; Eddaoudi, M.; Zaworotko, M. J. *J. Am. Chem. Soc.* **2012**, *134*, 928−933.

(31) Shultz, A. M.; Farha, O. K.; Hupp, J. T.; Nguyen, S. T. *Chem. Sci.* **2011**, *2*, 686−689.

(32) Yang, X. L.; Xie, M. H.; Zou, C.; He, Y. B.; Chen, B. L.; O'Keeffe, M.; Wu, C. D. *J. Am. Chem. Soc.* **2012**, *134*, 10638−10645.

(33) Mackintosh, H. J.; Budd, P. M.; McKeown, N. B. *J. Mater. Chem.* **2008**, *18*, 573−578.

(34) Schmidt, J.; Werner, M.; Thomas, A. *Macromolecules* **2009**, *42*, 4426−4429.

(35) Yuan, D. Q.; Lu, W. G.; Zhao, D.; Zhou, H. C. *Adv. Mater.* **2011**, *23*, 3723−3725.

(36) Konstas, K.; Taylor, J. W.; Thornton, A. W.; Doherty, C. M.; Lim, W. X.; Bastow, T. J.; Kennedy, D. F.; Wood, C. D.; Cox, B. J.; Hill, J. M.; Hill, A. J.; Hill, M. R. *Angew. Chem., Int. Ed.* **2012**, *51*, 6639−6642.

(37) Hauser, B. G.; Farha, O. K.; Exley, J.; Hupp, J. T. *Chem. Mater.* **2013**, *25*, 12−16.

(38) Wang, X. S.; Liu, J.; Bonefont, J. M.; Yuan, D. Q.; Thallapally, P. K.; Ma, S. Q. . *Chem. Commun.* **2013**, *49*, 1533−1535.

(39) Davoras, E. M.; Coutsolelos, A. G. *J. Inorg. Biochem.* **2003**, *94*, 161−170.

(40) Merlau, M. L.; Cho, S. H.; Sun, S. S.; Nguyen, S. T.; Hupp, J. T. *Inorg. Chem.* **2005**, *44*, 5523−5529.

(41) Monfared, H. H.; Aghapoor, V.; Ghorbanloo, M.; Mayer, P. *Appl. Catal., A* **2010**, *372*, 209−216.

(42) Nam, W.; Kim, I.; Lim, M. H.; Choi, H. J.; Lee, J. S.; Jang, H. G. *Chem. - Eur. J.* **2002**, *8*, 2067−2071.

(43) Srour, H.; Le Maux, P.; Simonneaux, G. *Inorg. Chem.* **2012**, *51*, 5850−5856.

(44) Zhou, X. T.; Ji, H. B.; Xu, H. C.; Pei, L. X.; Wang, L. F.; Yao, X. D. *Tetrahedron Lett.* **2007**, *48*, 2691−2695.

(45) The Fe-metallated PPOPs show poor reactivity toward epoxidation with 2-(*tert*-butylsulfonyl)iodosylbenzene, *tert*-butyl hydroperoxide, and hydrogen peroxide. Direct synthesis of Mn-PPOP from Mn(porphyrin) monomers was not successful.

(46) Song, F. J.; Wang, C.; Falkowski, J. M.; Ma, L. Q.; Lin, W. B. *J. Am. Chem. Soc.* **2010**, *132*, 15390−15398.

(47) Song, F. J.; Wang, C.; Lin, W. B. *Chem. Commun.* **2011**, *47*, 8256−8258.

(48) Havare, N.; Plattner, D. A. *Org. Lett.* **2012**, *14*, 5078−5081.

(49) Venturello, C.; Gambaro, M. *J. Org. Chem.* **1991**, *56*, 5924−5931.

(50) Walling, C.; Eltaliawi, G. M.; Amarnath, K. *J. Am. Chem. Soc.* **1984**, *106*, 7573−7578.

(51) Colclough, R. O.; Gee, G.; Higginson, W. C. E.; Jackson, J. B.; Litt, M. *J. Polym. Sci.* **1959**, *34*, 171−179.

(52) Koumura, K.; Satoh, K.; Kamigaito, M. *Macromolecules* **2008**, *41*, 7359−7367.

(53) Wang, J. S.; Matyjaszewski, K. *J. Am. Chem. Soc.* **1995**, *117*, 5614−5615.

(54) Nam, W.; Lee, H. J.; Oh, S. Y.; Kim, C.; Jang, H. G. *J. Inorg. Biochem.* **2000**, *80*, 219−225.

(55) Xia, Q. H.; Ge, H. Q.; Ye, C. P.; Liu, Z. M.; Su, K. X. *Chem. Rev.* **2005**, *105*, 1603−1662.

(56) de Sousa, A. N.; de Carvalho, M. E. M. D.; Idemori, Y. M. *J. Mol. Catal. A: Chem.* **2001**, *169*, 1−10.

(57) Elemans, J. A. A. W.; Bijsterveld, E. J. A.; Rowan, A. E.; Nolte, R. J. M. *Eur. J. Org. Chem.* **2007**, *2007*, 751−757.